Deep Learning Image Analysis of Macular Optical Coherence Tomography Angiography Images for Detection of Progression in Glaucoma

Aylin Mousavian
Department of Computer Science
California State University, Los Angeles
Los Angeles, CA, USA
amousav2@calstatela.edu

Jabiz Jarkaneh
Department of Public Health
University of the West of England
Bristol, England, UK
jabizjarganeh@gmail.com

Mohammad Pourhomayoun
Department of Computer Science
California State University, Los Angeles
Los Angeles, CA, USA
mpourho@calstatela.edu

Manveen Kaur
Department of Computer Science
California State University, Los Angeles
Los Angeles, CA, USA
mkaur39@calstatela.edu

Rohan Chatterjee
Department of Computer Science
California State University, Los Angeles
Los Angeles, CA, USA
rchatte@calstatela.edu

Sajad Besharati
Stein Eye Institute
University of California, Los Angeles
Los Angeles, CA, USA
abesharati@mednet.ucla.edu

Kouros Nouri-Mahdavi
Stein Eye Institute
University of California, Los Angeles
Los Angeles, CA, USA
nouri-mahdavi@jsei.ucla.edu

Navid Amini
Department of Computer Science
California State University, Los Angeles
Los Angeles, CA, USA
namini@calstatela.edu

***Abstract*— Optical Coherence Tomography Angiography (OCTA) is a new, non-invasive imaging modality for visualizing retinal capillaries for the diagnosis and management of multiple eye-related diseases. Glaucoma is one such disease, caused by the loss of retinal ganglion cells, which if progressed and not treated in time, will eventually lead to blindness. In this study, we present an innovative approach based on Convolutional Neural Networks (CNNs) to detect glaucoma progression. Our progression detection method is composed of five major steps: vessel segmentation, thick vessel masking, Otsu thresholding, super-pixel extraction, and measurement of macular microvascular density. Microvascular density measurements within predefined super pixels are compared between baseline and follow-up OCTA scans of 10 glaucoma patients. Our analysis demonstrates the effectiveness of our approach in distinguishing patients with progressive glaucoma from those whose glaucoma is stable. Our study offers a comprehensive assessment of microvascular vessel density dropouts observed in glaucomatous eyes over time, which enables early detection of disease progression. With proper management and timely treatment for patients with progressive glaucoma, vision loss can be slowed or prevented.**

Keywords—Optical Coherence tomography angiography, glaucoma progression detection, convolutional neural networks, vessel segmentation, microvascular vessel density measurement.

I. Introduction

Retinal degenerative diseases are prevalent among aging generations [1]. The vascular system plays an essential role in the health and function of the retina. The ocular blood flow system provides oxygen and nutrients to the retina, which is essential for maintaining vision, and its reduction has also been proposed to have a role in glaucoma's pathogenesis. Glaucoma is a multi-factorial disease and one of the most common reasons for vision loss in the world. There exists a strong association between a reduction in vascular perfusion and the presence of glaucoma [2]-[5]. There is a strong hypothesis that vascular factors such as decreased vessel density is significantly associated with the severity of visual field damage independent of structural damage. Visual field loss is conventionally considered the reference standard for determining the stage of glaucoma. However, visual field testing is subjective, prone to noise, and has modest repeatability. Recent studies suggest that reduction in vessel density may be a better indicator to track the progression of glaucoma [4]-[7].

One major advantage of OCTA imaging is its ability to analyze retinal vascular layers in deeper layers, where changes of glaucoma-induced vascular occur. Analysis of OCTA could better represent vascular structures and potentially enhance understanding of retinal impairments [6]. In order to substantiate the vascular hypothesis of glaucoma, a limited number of studies have been conducted to investigate the association between glaucoma progression and decreased blood flow in retinal vessels [7]. These investigations report changes in blood vessels located in the peripapillary area, optic disc, and macular area in glaucoma eyes in comparison with normal eyes [8], [9]. By extracting microvascular structures such as Superficial Vascular Complexes (SVC) and Deep Vascular Complexes (DVC) [10]-[11], from different OCTA depth-layers, one can obtain corresponding projections to observe respective variations in capillary levels [12]. Fig. 1 Shows the inner retinal vascular plexus including both SVC and DVC on macular OCTA images of two glaucoma patients. The inner retina extended from 3μm below the internal limiting membrane to the outer boundary of the outer plexiform layer [2], [13]-[14].

As vessel density is a critical parameter in advancement glaucoma, OCTA offers superior details of vessel visualization in order to perform vessel density measurements. Recently, Suh et al. [15] reported that decreased deep layer vessel density plays a substantial role in glaucoma progression; therefore, with the aid of vessel segmentation methods, deep layer vessel density is

obtained in order to calculate microvascular vessel density [16]-[19].

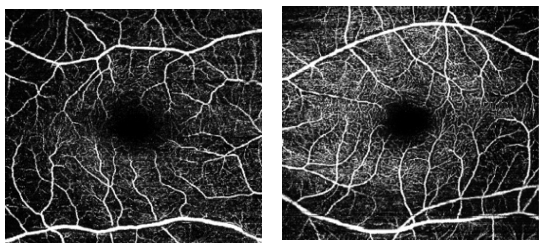

Fig. 1. The inner retina vascular plexus including Superficial Vascular Complexes and Deep Vascular Complexes.

Over the past two decades, numerous retinal vessel segmentation methods have been developed, categorized into two groups: supervised and unsupervised methods. Supervised retinal vessel segmentation techniques rely on pixel classification of vessels and non-vessels through a trained model and require an image dataset to train the model in order to obtain images of segmented vessels. Unsupervised retinal vessel segmentation methods require no prior information to segment the vessel. These methods are based on pixel tracking information or filtering scheme such as vessel tracking and matching filtering [20]-[25]. Recent vessel segmentation approaches aim at employing Convolutional Neural Networks (CNNs) [24], with the main challenge being the lack of adequate datasets for validation. Ma and colleagues apply CNN blocks for feature extraction to effectively segment retinal vessels using OCTA dataset ROSE into thick and thin vessels. Furthermore, they release the ROSE dataset, annotated with retinal microvascular network details [2], to the public to support OCTA research.

In our work, we leverage the ROSE dataset, proposing a novel method for glaucoma progression detection [25]. Our segmentation approach is based on CNNs [26], known for their excellence in semantic image segmentation and classification [27]-[29]. To improve efficiency and accuracy, we adopt a U-Net-based [30]-[33] fully convolutional neural network architecture proposed in [2] for retinal vessel segmentation into thick and thin vessels. We underscore the significance of decrease in macular vessel density, which has been reported in glaucomatous eyes in conjunction with thinning of the ganglion cell complex, and hence, the loss of ganglion cells [6], [14]. A novel approach is proposed for detecting glaucoma progression and is evaluated on images acquired from 10 patients with glaucomatous eyes. We conduct experiments to assess the utility of our approach in detecting glaucoma progression. Our proposed approach yields outstanding performance in distinguishing progressive eyes from stable ones.

The rest of the paper is organized as follows. Following introduction, Section II summarizes a number of related works, while Section III introduces preliminary notions concerning the proposed glaucoma progression detection method and presents our CNN based approach. Experimental results of the proposed method are presented in Section IV. Finally, Section V concludes this study.

II. Related Work

Significant advancements have occurred in glaucoma progression detection [34] and glaucoma detection through deep learning using fundus images [35]. Chen et al. present a method utilizing deep CNNs to perform feature learning and facilitate the detection of glaucoma. Their method aims to automatically learn relevant features from retinal fundus images in order to assist in the glaucoma diagnosis [36].

Zhang and associates [34] introduce a novel method for glaucoma progression detection using trend analysis of the thickness of the retinal nerve fiber layer (NFL) and ganglion cell complex (GCC) measured by OCT and visual field (VF). The investigators define progression as a significant negative trend in either NFL or GCC thickness. Based on results, OCT-based thickness measures are more sensitive than VF in detecting progression in glaucoma.

In [37], Bowd and colleagues develop a deep learning image analysis of OCTA measured vessel density to distinguish glaucoma eyes from healthy eyes. They evaluate the classification performance of the VGG16 CNN applied to OCTA images against Gradient Boost Classifier (GBC) model utilizing vessel density measurements. Their findings indicate substantial improvement in classification accuracy when using CNN model based on vessel density in comparison to GBC model. In [38] Mohammadzadeh et al. discuss a five-year study of glaucoma progression detection of macular OCTA with deep learning model. Glaucoma progression is determined based on specific visual field mean deviation rates. The study uses a customized CNN with a multi-layer perceptron classifier for classification. The authors' findings suggest that deep learning models demonstrate high performance in detecting glaucoma progression based on longitudinal macular OCTA images, potentially offering improved detection accuracy comparing to a logistic regression model.

Khalil and associates [39] provide various machine learning approaches for both glaucoma detection and prediction, they also investigate preprocessing methodologies to enhance the quality of OCT images as well as feature extraction methods to simplify data for classification. Their study emphasizes the pivotal role of feature extraction in achieving the accuracy of 85% in glaucoma detection.

In recent years, there has been a notable lack of comprehensive research on glaucoma progression detection using OCTA images. Existing methods predominantly rely on parameters such as visual field, retinal nerve fiber layer thickness and ganglion cell measurements utilizing conventional OCT images as their primary focus. Recent literature indicates a notable gap in the investigation of glaucoma progression detection through the analysis of macular thin vessel density. In response, our study aims to investigate a new method based on thin vessel density measurements derived from OCTA images.

III. Methods

A. Dataset

We utilize the ROSE dataset that has been introduced in [2]. The ROSE dataset consists of total of 117 OCTA images including 39 subjects with the mean (SD) age of 68.4 (7.4). All

scans are captured by the Optovue OCTA device (Optovue, Fremont, CA, USA) [33] equipped with AngioVue software, with the resolution of 304×304 pixels. This dataset contains both SVC and DVC angiograms of each participant. The ROSE dataset is employed for training our proposed method, and its performance is assessed using various image datasets. The testing dataset, consisting of OCTA images of patients with one 12-month follow up visit with varying degrees of glaucoma progression is provided by the UCLA Stein Eye Institute.

The mean (SD) age of the patients in the test set is 63.5 (20) years. Baseline scans acquired using the Optovue OCTA device, featuring an image resolution of 912×912 pixels. These scans cover a 6×6 mm^2 area centered on the fovea and include both SVC and DVC angiograms for each participant. The follow-up scans are automatically aligned to the baseline scan based on retinal vessel trajectories to ensure the measurements are derived from same location [34].

B. Derivation of vessel density

In this section, we detail a CNN-based pipeline to detect glaucoma progression using OCTA scans based on retinal vessel segmentation. The pipeline has five major stages as illustrated in Fig. 2. In the first stage, after image preprocessing, we detect and segment thick vessels using U-shape CNN networks. In stage 2, we proceed to mask thick vessels from the original OCTA image to obtain thin vessels of the macula. Subsequently, at stage 3, we apply the Otsu-thresholding method to intensify thin vessels. Stage 4 involves the extraction of super-pixels from both baseline and follow-up OCTA images to be able to systematically measure thin vessel density. Finally, in stage 5, we measure thin vessel density as our biomarker to detect glaucoma progression.

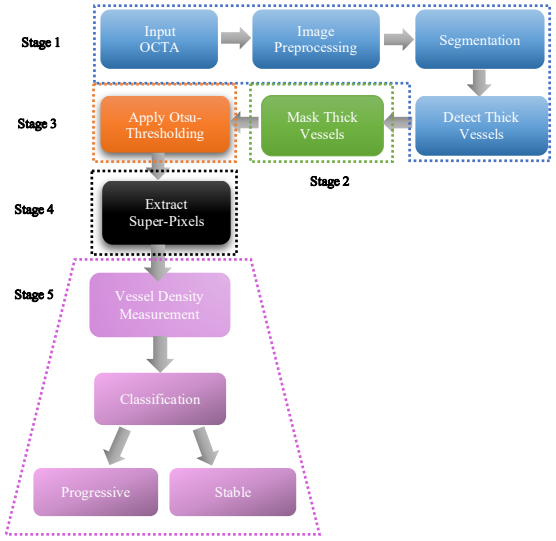

Fig. 2. Proposed pipeline for detection of glaucoma progression contains five major stages.

Throughout this article, we use the terms macular microvascular density and macular thin vessel density interchangeably.

The ROSE dataset is utilized during the training model to extract thick vessels. The definition of the term 'thick vessels' has been provided in [2]. According to our ophthalmologist collaborators, macular thick vessels likely exhibit minimal changes during glaucoma progression, whereas major changes would occur primarily in thin vessels. By extracting and masking thick vessels, we can effectively quantify the density of thin vessels, in order to detect glaucoma progression. Thick vessel extraction is originally derived by the method proposed by Ma et al. [2] containing a U-shape network architecture including five symmetric encoder/decoder blocks.

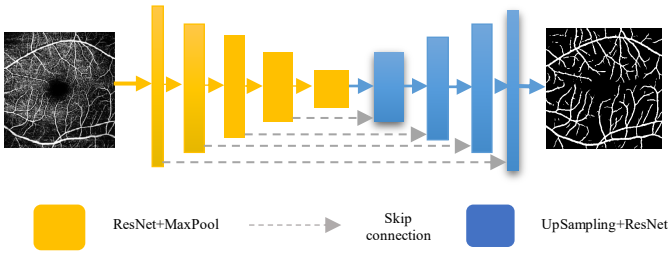

Fig. 3. Detecting thick vessels on input images.

A sample output of thick vessel detection stage is presented in Fig. 3. Extracted thick vessel images are masked from original OCTA images, resulting in OCTA images with only thin macular vessels (Fig. 4).

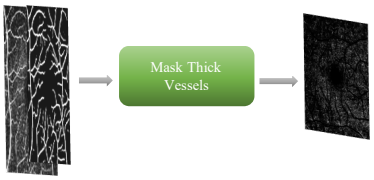

Fig. 4. Masking thick vessels from Original OCTA image.

Next, we measure blood vessel density from masked OCTA output images. Based on the recommendation of our ophthalmologist collaborators, the blood vessel density will likely change as glaucoma progresses. Thin vessel density of baseline and follow-up is calculated and compared to capture progression of glaucoma in a specific eye. We employ the Simple Linear Iterative Clustering (SLIC) [40] method to segment OCTA images obtained from previous stage into 100 super-pixels with equal size. A super-pixel is defined as a group of pixels that share common characteristics. The utilization of super-pixels is motivated by their ability to reduce sensitivity to noise and simplify the complexity of vessel density measurement. To calculate super-pixels vessel density, we convert 3-channel RGB images to grayscale images. This strategy needs binarization thresholding [41] which involves an algorithm to clearly generate an OCTA image to assign each pixel value to either white or black in order to obtain binary image [41]-[42]. In our method, Otsu-thresholding is applied to calculate the optimal threshold, to separate the vessels from the background in an OCTA image. Otsu-thresholding is based on pixel density; if the value of specific pixel of input image is greater than the threshold the corresponding pixel is marked as white, and if the input pixel intensity is less than or equal the threshold, that specific pixel on output image is marked black.

The Otsu-thresholding method has three steps as follow:

- Compute image histogram,
- Obtain the threshold value as T,
- Replace pixels into white pixel where saturation is higher than T and into black in opposite case.

After obtaining the histogram, the image is partitioned into two clusters with the threshold defined by minimizing the weighted variance of the classes depicted by $\sigma_{\omega}^2(t)$. The whole equation can be described as follows:

$$\sigma_{\omega}^2(t) = \omega_1(t)\sigma_1^2(t) + \omega_2(t)\sigma_2^2(t), \quad (1)$$

where $\omega_1(t)$, $\omega_2(t)$ represents the probabilities of two classes divided by a threshold T, which takes values within the range of 0 to 255 inclusively. As illustrated in [43], there are two options to obtain the threshold, the first one is to minimize within-class variance denoted above as $\sigma_{\omega}^2(t)$, the second is to maximize between-class variance using expression as follow:

$$\sigma_b^2(t) = \omega_1(t)\omega_2(t)[\mu_1(t) - \mu_2(t)],^2 \quad (2)$$

where μ_i is the mean value of each class of i.

It should be noted that the image can be represented as intensity function $f(x, y)$, where values are in grayscale level. If i represent the quantity of pixels with a specific grayscale level, and n denotes the total number of pixels in the image. Thus, the probability of grayscale level i is calculated as: $P(i) = \frac{n_i}{n}$. The probability P is calculated for each pixel ranging from 0 to 255, in two separated clusters C_1 and C_2 using probability functions as $P(i)$.

$$\omega_1(t) = \sum_{i=1}^{t} P(i) \quad (3)$$

$$\omega_2(t) = \sum_{i=t+1}^{I} P(i) \quad (4)$$

The pixel intensity values for the C_1 are in $[1, t]$ and for C_2 are in $[t + 1, I]$, where I is the maximum pixel value 255. Afterwards, the mean value for C_1, C_2 is obtained as $\mu_1(t)$ and $\mu_2(t)$, respectively;

$$\mu_1(t) = \sum_{i=1}^{t} \frac{iP(i)}{\omega_1(t)} \quad (5)$$

$$\mu_2(t) = \sum_{i=t+1}^{I} \frac{iP(i)}{\omega_2(t)} \quad (6)$$

where, μ_i is the mean value belonging to each class.

The final threshold is calculated for every pair of test-set OCTA images and applied to assign pixels to a proper value based on the Otsu algorithm to optimize image contrast [43]. This method preserves true blood flow, simplifying the quantitative measurements of vessel density for every super-pixel in the next stage. In this stage, SLIC algorithm [40] will be applied to the output OCTA images from the previous stage. The SLIC algorithm obtains super-pixels with regular size as depicted in Fig. 5. Every super-pixel has been generated with inner connectivity and it is guaranteed that each pixel is included in one specific super-pixel. The main purpose of segmenting OCTA images into super-pixels is vessel density measurement on baseline OCTA image in comparison with follow-up OCTA image from same eye. The difference between super-pixels density is used to detect glaucoma progression in a specific eye.

Fig. 5. Appling SLIC, to segment OCTA image into 100 super-pixel.

IV. Experiments

We evaluate the performance of our innovative glaucoma progression detection method through extensive experiments. We apply a test-set, including baseline and follow-up scans from 10 glaucoma patients with varying severity of glaucoma. Applying our method to these OCTA images enable us to perform a comparison of vessel density values for corresponding super-pixels in baseline and follow-up scans. The results are promising, demonstrating the method's precision in detecting progressive glaucoma. Patients with deteriorating conditions exhibit substantial changes in vessel density, while stable conditions show minimal changes. This suggests the potential value of our approach for monitoring glaucoma progression over time and assessing treatment effectiveness.

Scatter plots and line charts are utilized in order to analyze vessel density measurements in a detailed manner across 100 super-pixels in both baseline and follow-up scans.

A. Evaluation Metrics

In order to obtain a thorough and comprehensive evaluation of the first stage of the proposed method, the accuracy metric is utilized to represent the performance of thick vessel segmentation. The first stage of the method achieves an accuracy of 97.4% in segmenting thick vessels, as shown in Fig. 6. The yellow image represents the ground truth, annotated by ophthalmologists to grade thick vessel segmentation in OCTA images at the pixel level. The pink image corresponds to the output of predicted thick vessel segmentation with our method, while the white image depicts the merged of annotated thick vessels and predicted thick vessels.

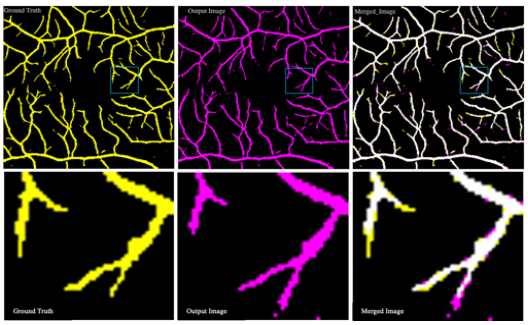

Fig. 6. Ground truth (yellow); predicted (pink); merged image (white).

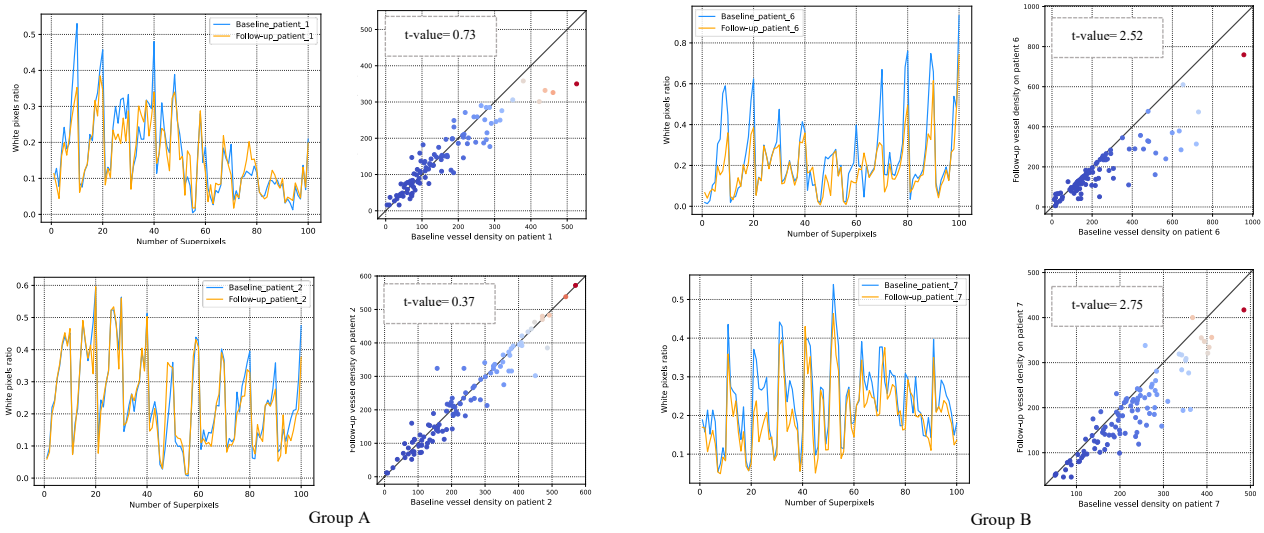

Fig. 7. Group A contains stable glaucoma patients with t-value lower than 1 on patient 1 and patient 2. Scatter plot and line chart represent minimal change on thin vessel density comparing baseline and follow-up, whereas group B represent significant change on thin vessel density which means progressive glaucoma in patient 6 and patient 7, comparing baseline and follow-up.

For the purpose of analyzing glaucoma progression from OCTA images, we utilize the t-value patterns as the basis for identifying a significant change in vessel density between the baseline and follow-up OCTA images. In other words, the t-value is calculated using the following equation:

$$\text{t-value} = \frac{\bar{X}_1 + \bar{X}_2}{\sqrt{\frac{S_1^2}{n_1} + \frac{S_2^2}{n_2}}} \qquad (7)$$

B. *Experimental Results*

In this section, we implement the proposed method on a test-set comprising images from patients at varying glaucoma degrees including both baseline and follow-up scans. Each image is resized into a grayscale image with 304×304 pixels. Fig. 7 demonstrate samples with progressive and stable (non-progressive) glaucoma. In the left panel of figure, the vessel density values for two patients whose glaucoma is stable is visualized by line charts and scatterplots with the reference of y=x. points on this line represent super-pixels whose vessel density did not change over time, which is indicative of glaucoma's stability. The right panel of the figure contains similar visualizations for two sample patients whose glaucoma is progressive and as a result, the follow-up line charts in yellow color are noticeably below their blue counterparts. Moreover, the skewness of points below the y=x line in the scatterplots signals a decline in vessel density over time, pointing out the progression of glaucoma in these two patients. The vessel density analysis of the super-pixels in group A including patient 1 and 2, suggests that their condition is stable, and glaucoma is considered non-progressive. To further elaborate our findings, such a small t-value of 0.73 for patient 1 and 0.37 for patient 2, confirm that there has been only minor change in the vessel density, providing additional proof of consistency in our results.

Upon comparison of the baseline and follow-up data for group B consisting of patient 6 and 7, there is evidence of progression of glaucoma. t-values of 2.52 and 2.75 for patient 6 and patient 7 represent a significant change between the follow-up and baseline images. This suggests that the disease has progressed over time in these patients.

In general, the greater the t-values the higher the probability that changes in vessel density between baseline and follow-up is not due to random fluctuations in vessel density.

For this testing dataset of baseline and follow-up images, our method achieves perfect progression detection performance. This outcome strongly supports the hypothesis that a decline in thin vessel density in deep vascular complexes of the macula using OCTA images is a robust indicator of glaucoma progression. In our subsequent analysis, we categorize the test-set patients into two distinct groups based on t-values: the progressive glaucoma group for cases with t-values greater than 1, and stable (non-progressive) group for cases with t-values less than 1 as depicted in Fig. 8.

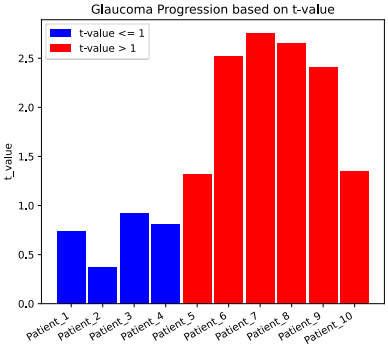

Fig. 8. Bar-chart illustration of glaucoma status categorized as progressive and stable.

V. Conclusions

Rate of disease progression is one of the most important factors determining the risk of visual disability or blindness in glaucoma, and the evaluation of rate of progression in routine care is often recommended for glaucoma management. In this paper, we introduce a novel five-stage method for detecting glaucoma progression. Our approach includes a U-Net-based architecture utilizing ResNet blocks as the backbone for thick vessel segmentation. After removing the thick vessels from the OCTA images, we apply Otsu-thresholding to enhance the visibility of thin capillaries, allowing for precise vessel density measurement in glaucoma progression detection. Our comprehensive experiments on the test-set demonstrate the outstanding performance of our approach in capturing glaucoma progression. We further support our findings by conducting a t-value analysis on thin vessel variations within the test-set in order to confirm our hypothesis. This study underscore the potential of retinal microvascular-based analysis in detecting glaucoma progression, where small capillaries play a pivotal role in glaucoma progression detection. The outcomes of our study highlight that the proposed approach excels in efficiently assessing the glaucoma progression status during its initial stages. This framework holds the potential to enhance detection of glaucoma progression. Accordingly, more rigorous treatments can be considered for those whose glaucoma is progressing and are at a higher risk of blindness form glaucoma.

References

[1] N. Amini *et al.*, "Influence of the Disc–Fovea Angle on Limits of RNFL Variability and Glaucoma Discrimination," *Investig. Opthalmology Vis. Sci.*, vol. 55, no. 11, p. 7332, Nov. 2014, doi: 10.1167/iovs.14-14962.

[2] Y. Ma *et al.*, "ROSE: A Retinal OCT-Angiography Vessel Segmentation Dataset and New Model," *IEEE Trans. Med. Imaging*, vol. 40, no. 3, pp. 928–939, Mar. 2021, doi: 10.1109/TMI.2020.3042802.

[3] S. Nowroozizadeh *et al.*, "Influence of Correction of Ocular Magnification on Spectral-Domain OCT Retinal Nerve Fiber Layer Measurement Variability and Performance," *Investig. Opthalmology Vis. Sci.*, vol. 55, no. 6, p. 3439, Jun. 2014, doi: 10.1167/iovs.14-13880.

[4] A. Yarmohammadi et al., "Relationship between Optical Coherence Tomography Angiography Vessel Density and Severity of Visual Field Loss in Glaucoma," *Ophthalmology*, vol. 123, no. 12, pp. 2498–2508, Dec. 2016, doi: 10.1016/j.ophtha.2016.08.041.

[5] M. Madhumalini and T. Meera Devi, "Detection of Glaucoma from Fundus Images Using Novel Evolutionary-Based Deep Neural Network," *Journal of Digital Imaging*, vol. 35, pp. 1008–1022, 2022.

[6] N. Amini *et al.*, "The Relationship of the Clinical Disc Margin and Bruch's Membrane Opening in Normal and Glaucoma Subjects," *Investig. Opthalmology Vis. Sci.*, vol. 57, no. 3, p. 1468, Mar. 2016, doi: 10.1167/iovs.15-18382.

[7] M. S. Sarabi *et al.*, "3D Retinal Vessel Density Mapping With OCT-Angiography," *IEEE J. Biomed. Health Inform.*, vol. 24, no. 12, pp. 3466–3479, Dec. 2020, doi: 10.1109/JBHI.2020.3023308.

[8] Y.-C. Tham, X. Li, T. Y. Wong, H. A. Quigley, T. Aung, and C.-Y. Cheng, "Global Prevalence of Glaucoma and Projections of Glaucoma Burden through 2040," *Ophthalmology*, vol. 121, no. 11, pp. 2081–2090, Nov. 2014, doi: 10.1016/j.ophtha.2014.05.013.

[9] C. Lommatzsch, K. Rothaus, J. M. Koch, C. Heinz, and S. Grisanti, "Vessel Density in Glaucoma of Different Entities as Measured with Optical Coherence Tomography Angiography," *Clin. Ophthalmol. Auckl. NZ*, vol. 13, pp. 2527–2534, 2019, doi: 10.2147/OPTH.S230192.

[10] Danilo Andrade *et al.*, "OCTA Multilayer and Multisector Peripapillary Microvascular Modeling for Diagnosing and Staging of Glaucoma," *Transl. Vis. Sci. Technol.*, vol. 9, p. 58, 2020.

[11] T. T. Hormel *et al.*, "Plexus-specific retinal vascular anatomy and pathologies as seen by projection-resolved optical coherence tomographic angiography," *Prog. Retin. Eye Res.*, vol. 80, p. 100878, Jan. 2021, doi: 10.1016/j.preteyeres.2020.100878.

[12] M. E. Hartnett, J. J. Weiter, G. Staurenghi, and A. E. Elsner, "Deep Retinal Vascular Anomalous Complexes in Advanced Age-related Macular Degeneration," *Ophthalmology*, vol. 103, no. 12, pp. 2042–2053, Dec. 1996, doi: 10.1016/S0161-6420(96)30389-8.

[13] J. Zhang *et al.*, "3D Shape Modeling and Analysis of Retinal Microvasculature in OCT-Angiography Images," *IEEE Trans. Med. Imaging*, vol. 39, no. 5, pp. 1335–1346, May 2020, doi: 10.1109/TMI.2019.2948867.

[14] J. P. Campbell *et al.*, "Detailed Vascular Anatomy of the Human Retina by Projection-Resolved Optical Coherence Tomography Angiography," *Sci. Rep.*, vol. 7, no. 1, p. 42201, Feb. 2017, doi: 10.1038/srep42201.

[15] M. H. Suh *et al.*, "Deep Retinal Layer Microvasculature Dropout Detected by the Optical Coherence Tomography Angiography in Glaucoma," *Ophthalmology*, vol. 123, no. 12, pp. 2509–2518, Dec. 2016, doi: 10.1016/j.ophtha.2016.09.002.

[16] K. K. W. Chan, F. Tang, C. C. Y. Tham, A. L. Young, and C. Y. Cheung, "Retinal vasculature in glaucoma: a review," *BMJ Open Ophthalmol.*, vol. 1, no. 1, p. e000032, 2017, doi: 10.1136/bmjophth-2016-000032.

[17] N. Patton, T. Aslam, T. Macgillivray, A. Pattie, I. J. Deary, and B. Dhillon, "Retinal vascular image analysis as a potential screening tool for cerebrovascular disease: a rationale based on homology between cerebral and retinal microvasculatures," *J. Anat.*, vol. 206, no. 4, pp. 319–348, Apr. 2005, doi: 10.1111/j.1469-7580.2005.00395. x.

[18] D. Romaus-Sanjurjo *et al.*, "Alzheimer's Disease Seen through the Eye: Ocular Alterations and Neurodegeneration," *Int. J. Mol. Sci.*, vol. 23, no. 5, p. 2486, Feb. 2022, doi: 10.3390/ijms23052486.

[19] D. Marin, A. Aquino, M. E. Gegundez-Arias, and J. M. Bravo, "A new supervised method for blood vessel segmentation in retinal images by using gray-level and moment invariants-based features," *IEEE Trans. Med. Imaging*, vol. 30, no. 1, pp. 146–158, Jan. 2011, doi: 10.1109/TMI.2010.2064333.

[20] A. Galdran, A. Anjos, J. Dolz, H. Chakor, H. Lombaert, and I. B. Ayed, "State-of-the-art retinal vessel segmentation with minimalistic models," *Sci. Rep.*, vol. 12, no. 1, p. 6174, Apr. 2022, doi: 10.1038/s41598-022-09675-y.

[21] J. Almotiri, K. Elleithy, and A. Elleithy, "Retinal Vessels Segmentation Techniques and Algorithms: A Survey," *Appl. Sci.*, vol. 8, no. 2, p. 155, Jan. 2018, doi: 10.3390/app8020155.

[22] U-Net: Convolutional Networks for Biomedical Image Segmentation, Olaf Ronneberger, Philipp Fischer, and Thomas Brox, "U-Net: Convolutional Networks for Biomedical Image Segmentation," *International Conference on Medical Image Computing and Computer-Assisted Intervention*, pp. 234–241, 2015.

[23] Ali Can, Hong Shen, Turner, Tanenbaum, and Roysam, "Rapid automated tracing and feature extraction from retinal fundus images using direct exploratory algorithms," *IEEE Trans. Inf. Technol. Biomed.*, vol. 3, no. 2, pp. 125–138, Jun. 1999, doi: 10.1109/4233.767088.

[24] J. V. B. Soares, J. J. G. Leandro, R. M. Cesar Júnior, H. F. Jelinek, and M. J. Cree, "Retinal vessel segmentation using the 2-D Gabor wavelet and supervised classification," *IEEE Trans. Med. Imaging*, vol. 25, no. 9, pp. 1214–1222, Sep. 2006, doi: 10.1109/tmi.2006.879967.

[25] H. Abdushkour *et al.*, "Enhancing fine retinal vessel segmentation: Morphological reconstruction and double thresholds filtering strategy," *PloS One*, vol. 18, no. 7, p. e0288792, 2023, doi: 10.1371/journal.pone.0288792.

[26] Z. Zhou, M. M. Rahman Siddiquee, N. Tajbakhsh, and J. Liang, "UNet++: A Nested U-Net Architecture for Medical Image Segmentation," in *Deep Learning in Medical Image Analysis and Multimodal Learning for Clinical Decision Support*, vol. 11045, D. Stoyanov, Z. Taylor, G. Carneiro, T. Syeda-Mahmood, A. Martel, L. Maier-Hein, J. M. R. S. Tavares, A. Bradley, J. P. Papa, V. Belagiannis, J. C. Nascimento, Z. Lu, S. Conjeti, M. Moradi, H. Greenspan, and A. Madabhushi, Eds., in Lecture Notes in Computer Science, vol. 11045. , Cham: Springer International Publishing, 2018, pp. 3–11. doi: 10.1007/978-3-030-00889-5_1.

[27] Y. LeCun, K. Kavukcuoglu, and C. Farabet, "Convolutional networks and applications in vision," in *Proceedings of 2010 IEEE International Symposium on Circuits and Systems*, Paris, France: IEEE, May 2010, pp. 253–256. doi: 10.1109/ISCAS.2010.5537907.

[28] L.-C. Chen, G. Papandreou, I. Kokkinos, K. Murphy, and A. L. Yuille, "DeepLab: Semantic Image Segmentation with Deep Convolutional Nets, Atrous Convolution, and Fully Connected CRFs," *IEEE Trans. Pattern Anal. Mach. Intell.*, vol. 40, no. 4, pp. 834–848, Apr. 2018, doi: 10.1109/TPAMI.2017.2699184.

[29] S. M. Anwar, M. Majid, A. Qayyum, M. Awais, M. Alnowami, and M. K. Khan, "Medical Image Analysis using Convolutional Neural Networks: A Review," *J. Med. Syst.*, vol. 42, no. 11, p. 226, Nov. 2018, doi: 10.1007/s10916-018-1088-1.

[30] Neural Information Processing Systems Foundation, Ed., *Advances in neural information processing systems 25: 26th Annual Conference on Neural Information Processing Systems 2012; December 3 - 6, 2012, Lake Tahoe, Nevada, USA*. Red Hook, NY: Curran, 2013.

[31] X.-X. Yin, L. Sun, Y. Fu, R. Lu, and Y. Zhang, "U-Net-Based Medical Image Segmentation," *J. Healthc. Eng.*, vol. 2022, pp. 1–16, Apr. 2022, doi: 10.1155/2022/4189781.

[32] N. Siddique, S. Paheding, C. P. Elkin, and V. Devabhaktuni, "U-Net and Its Variants for Medical Image Segmentation: A Review of Theory and Applications," *IEEE Access*, vol. 9, pp. 82031–82057, 2021, doi: 10.1109/ACCESS.2021.3086020.

[33] F. J. Freiberg, M. Pfau, J. Wons, M. A. Wirth, M. D. Becker, and S. Michels, "Optical coherence tomography angiography of the foveal avascular zone in diabetic retinopathy," *Graefes Arch. Clin. Exp. Ophthalmol.*, vol. 254, no. 6, pp. 1051–1058, Jun. 2016, doi: 10.1007/s00417-015-3148-2.

[34] X. Zhang *et al.*, "Comparison of Glaucoma Progression Detection by Optical Coherence Tomography and Visual Field," *Am. J. Ophthalmol.*, vol. 184, pp. 63–74, Dec. 2017, doi: 10.1016/j.ajo.2017.09.020.

[35] K. Jin *et al.*, "FIVES: A Fundus Image Dataset for Artificial Intelligence based Vessel Segmentation," *Sci. Data*, vol. 9, no. 1, p. 475, Aug. 2022, doi: 10.1038/s41597-022-01564-3.

[36] X. Chen, Y. Xu, S. Yan, D. W. K. Wong, T. Y. Wong, and J. Liu, "Automatic Feature Learning for Glaucoma Detection Based on Deep Learning," in *Medical Image Computing and Computer-Assisted Intervention – MICCAI 2015*, vol. 9351, N. Navab, J. Hornegger, W. M. Wells, and A. F. Frangi, Eds., in Lecture Notes in Computer Science, vol. 9351. , Cham: Springer International Publishing, 2015, pp. 669–677. doi: 10.1007/978-3-319-24574-4_80.

[37] C. Bowd et al., "Deep Learning Image Analysis of Optical Coherence Tomography Angiography Measured Vessel Density Improves Classification of Healthy and Glaucoma Eyes," Am. J. Ophthalmol., vol. 236, pp. 298–308, Apr. 2022, doi: 10.1016/j.ajo.2021.11.008.

[38] V. Mohammadzadeh et al., "Detection of Glaucoma Progression on Longitudinal Series of Macular Optical Coherence Tomography Angiography Maps with a Deep Learning Model," Iovs Investig. Ophthalmol. Vis. Sci., vol. 63, no. 7, Jun. 2022.

[39] T. Khalil, S. Khalid, and A. M. Syed, "Review of Machine Learning techniques for glaucoma detection and prediction," in 2014 Science and Information Conference, London, UK: IEEE, Aug. 2014, pp. 438–442. doi: 10.1109/SAI.2014.6918224.

[40] X. D. Bai, Z. G. Cao, Y. Wang, M. N. Ye, and L. Zhu, "Image segmentation using modified SLIC and Nyström based spectral clustering," *Optik*, vol. 125, no. 16, pp. 4302–4307, Aug. 2014, doi: 10.1016/j.ijleo.2014.03.035.

[41] N. Mehta *et al.*, "Impact of Binarization Thresholding and Brightness/Contrast Adjustment Methodology on Optical Coherence Tomography Angiography Image Quantification," *Am. J. Ophthalmol.*, vol. 205, pp. 54–65, Sep. 2019, doi: 10.1016/j.ajo.2019.03.008.

[42] N. Otsu, "A Threshold Selection Method from Gray-Level Histograms," *IEEE Trans. Syst. Man Cybern.*, vol. 9, no. 1, pp. 62–66, Jan. 1979, doi: 10.1109/TSMC.1979.4310076.

[43] R. Laiginhas, D. Cabral, and M. Falcão, "Evaluation of the different thresholding strategies for quantifying choriocapillaris using optical coherence tomography angiography," *Quant. Imaging Med. Surg.*, vol. 10, no. 10, pp. 1994–2005, Oct. 2020, doi: 10.21037/qims-20-340.